ELSEVIER

Contents lists available at ScienceDirect

Geochimica et Cosmochimica Acta

journal homepage: www.elsevier.com/locate/gca



Mid- and long-chain leaf wax δ^2H values in modern plants and lake sediments from mid-latitude North America



Ioana C. Stefanescu^{a,*}, Chandelle Macdonald^b, Craig S. Cook^b, David G. Williams^{b,c}, Bryan N. Shuman^a

- ^a Department of Geology and Geophysics, University of Wyoming, Laramie, WY, USA
- ^b The Stable Isotope Facility, University of Wyoming, Laramie, WY, USA
- ^c Department of Botany, University of Wyoming, Laramie, WY, USA

ARTICLE INFO

Article history: Received 27 June 2022 Accepted 3 November 2022 Available online 8 November 2022 Associate editor: Aaron F. Diefendorf

Keywords: Stable isotopes Leaf waxes Hydroclimate reconstructions

ABSTRACT

Compound-specific δ^2 H values of leaf wax *n*-alkanes are increasingly being used to infer past hydroclimates. However, differences in n-alkane production and apparent fractionation factors (ε_{app}) among different plant groups complicate the relationships between n-alkane δ^2 H values and those of environmental water. Mid- and long-chain n-alkanes in sedimentary archives (i.e., n- C_{23} and n- C_{29}) are thought to derive from aquatic and terrestrial plants, respectively, and track the isotopic composition of either lake water or precipitation. Yet, the relationship between n- C_{23} δ^2 H values and lake water δ^2 H values is not well constrained. Moreover, recent studies show that n-alkane production is greater in terrestrial plants than in aquatic plants, which has the potential to obscure n-alkane aquatic inputs to sedimentary archives. Here, we investigated n-alkane contributions to sedimentary archives from both aquatic and terrestrial plants by analyzing n-alkane δ^2 H values in plants and lake sediments at 29 sites across mid-latitude North America. We find that both aquatic and terrestrial plants synthesize n-C23 and that sedimentary n- C_{23} δ^2 H values parallel those of terrestrial plants and differ from those of aquatic plants. Our results indicate that across mid-latitude North America, both mid- and long-chain n-alkanes in lake sediments commonly derive from terrestrial higher plants challenging the assumption that submerged aquatic plants produce the n-C23-alkane preserved in lake sediments. Moreover, angiosperm and gymnosperm plants exhibit similar ϵ_{app} values between n-C $_{29}$ and mean annual precipitation (MAP) δ^2 H values across North America. Therefore, vegetation shifts between angiosperm and gymnosperm plants do not strongly affect ε_{app} values between n-C $_{29}$ and MAP. Our results show that both mid- and longchain *n*-alkanes track the isotopic composition of MAP in temperate North America.

© 2022 Elsevier Ltd. All rights reserved.

1. Introduction

Compound-specific hydrogen isotopic ratios of leaf wax n-alkanes are increasingly being used as proxies for past precipitation changes (Schefuß et al., 2005; Pagani et al., 2006; Aichner et al., 2010a; Tierney et al., 2011; Rach et al., 2014; Curtin et al., 2019; Puleo et al., 2020). Leaf wax n-alkanes are simple, unbranched, long-chain saturated organic compounds (formula: C_nH_{2n+2}) biosynthesized by plants at the leaf surface during leaf formation from alkanoic acids through the decarboxylation pathway (Jetter et al., 2006; Tipple et al., 2013; Sachse et al., 2010). A stable chemical configuration enables n-alkanes to preserve well in marine and freshwater sediments and facilitates extraction

E-mail address: istefane@uwyo.edu (I.C. Stefanescu).

and purification (Yang and Huang, 2003; Sessions et al., 2004; Schimmelmann et al., 2006; Diefendorf et al., 2015; Sessions, 2016). Depending on the plant growth environment, the hydrogen source of leaf wax *n*-alkanes may derive from canopy-intercepted precipitation, soil moisture, or lake water. Since precipitation is the ultimate hydrogen source, leaf wax *n*-alkanes have been shown to track the hydrogen isotopic signature of precipitation and have become proxies for studying past changes in environmental moisture (Sachse et al., 2004; Sachse et al., 2012; Tipple et al., 2013, McFarlin et al., 2019). Because different compounds may represent different moisture sources (e.g., lake water versus soil moisture), understanding the differences could further enhance reconstruction of multiple hydrologic processes such as soil or lake evaporation (Rach et al., 2014; Rach et al., 2017; Curtin et al., 2019).

n-Alkanes absolute abundances and relative abundances of the different chain lengths vary widely among plant types and among different environments (Ficken et al., 2000; Diefendorf et al., 2011;

 $[\]ast$ Corresponding author at: 1000 E University Ave., Science Initiative Bldg. Room 4234, Laramie, WY 82071, USA.

Feakins et al., 2016; Liu and Liu, 2016; Liu et al., 2017). For example, terrestrial broad leaf trees produce up to 300 times more *n*-alkanes per gram of dry leaf than shrubs and grasses (Freimuth et al., 2019), n-alkanes are up to 200 times more abundant in angiosperms than in gymnosperms (Diefendorf et al., 2011), and 30 times more abundant in terrestrial than aquatic plants (Dion-Kirschner et al., 2020). The distribution of *n*-alkane chain lengths also varies based on plant growth environment. Aquatic submerged and floating plants preferentially produce mid-chain homologues (n-C₂₁-n-C₂₅) (Ficken et al., 2000, Aichner et al., 2010b; Gao et al., 2011), while terrestrial plants maximally form long-chain homologues (>n-C₂₅) (Bush and McInerney, 2013). The difference in the most common chain lengths between aquatic and terrestrial plants has led to the use of the mid-chain n- C_{23} as proxy for lake water δ^2 H values and evapotranspiration (Nichols et al., 2006: Seki et al., 2011: Rach et al., 2014: Rach et al., 2017: Curtin et al., 2019; Puleo et al., 2020) and to the use of the longchain n-C₂₉-alkane as proxy for precipitation δ^2 H values (Schefuß et al., 2005; Pagani et al., 2006; Rach et al., 2014; Curtin et al., 2019; Puleo et al., 2020; Schartman et al., 2020). A challenge with this approach has been that most plants produce varying amounts of both mid- and long-chain *n*-alkanes (Ficken et al., 2000; Gao et al., 2011; Feakins et al., 2016; Wang et al., 2018; He et al., 2020), and the high production rates of all *n*-alkanes by terrestrial plants may dominate over aquatic sources even for mid-chain lengths (Freimuth et al., 2019; Dion-Kirschner et al., 2020).

Precipitation δ^2 H composition undergoes isotopic fractionation through soil or lake water evaporation, transpiration as well as during plant biosynthesis, which leads to a systematic difference between the δ^2 H values of *n*-alkanes relative to those of precipitation. This apparent fractionation factor (ϵ_{app}) varies as a function of chain length, as well as plant type, climatic conditions and geographic location (Sachse et al., 2012; Feakins et al., 2018; McFarlin et al., 2019). ε_{app} has been well described for the n- C_{29} alkane, enabling estimates of precipitation δ^2H values (Sachse et al., 2012; McFarlin et al., 2019). A recent global compilation of leaf wax δ^2 H values from sedimentary archives (McFarlin et al., 2019) confirmed a strong relationship ($r^2 = 0.8$) between n- C_{20} δ²H values and those of mean annual precipitation (MAP) with an average apparent fractionation factor, $\varepsilon_{C29/MAP}$, of -121% (s.d. = 18%o). However, ε_{app} between n- C_{23} and lake water has not been as widely constrained; the relationship ($r^2 = 0.4$) is much weaker than for n- C_{29} and MAP (McFarlin et al., 2019). Consequently, although n- C_{29} and n- C_{23} δ^2 H values are assumed to represent terrestrial and aquatic sources, and often treated as $\delta^2 H_{Terrestrial}$ and δ²H_{Aquatic}, respectively (Balascio et al., 2013; Rach et al., 2014), these relationships may be complex in many settings (McFarlin et al., 2019; Dion-Kirschner et al., 2020; He et al., 2020).

Models have been developed to differentiate the n-alkane sources (i.e., aquatic or terrestrial inputs) in sedimentary archives based on the relative abundances of mid- and long-chain n-alkanes (Ficken et al., 2000; Gao et al., 2011; Wang et al., 2018; Dion-Kirschner et al., 2020; Peaple et al., 2021). However, differences in n-alkane production between terrestrial and aquatic plants combined with different plant distributions in and around lakes presents a challenge to this approach (Diefendorf and Freimuth, 2017). A recent study from Greenland shows that n-alkane δ^2 H values and their distributions in sedimentary archives are more similar to those observed in terrestrial plants, and, therefore, mid-chain n-alkanes do not track lake water isotopic signatures at some sites in the high latitudes (Dion-Kirschner et al., 2020).

Given the need to elucidate the use of n- C_{23} -alkane as a proxy for lake water $\delta^2 H$ values in temperate regions, we analyzed the $\delta^2 H$ composition of mid- and long-chain n-alkanes in sediments, aquatic plants, and terrestrial plants across mid-latitude North

America. We investigate the potential leaf wax sources in lake sediments from the Rocky Mountains east to the Atlantic coast and evaluate the relationships between mid- and long-chain n-alkanes δ^2 H values and environmental waters.

2. Methods

2.1. Study sites and sample collection

Modern surface sediments, lake water, aquatic and terrestrial plants were collected in and around 29 lakes from across central and eastern United States during May and early June of 2018 (Fig. 1, Table 1, lakes numbered 1 through 29). The lakes span a large climatic gradient where mean annual air temperatures (MAAT) range from 5.4 to 19.5 °C. Mean annual precipitation (MAP) varies from 353 to 1431 mm/year and elevation from 11 to 2181 m (Table 1). MAAT and MAP were obtained using the Parameter-Elevation Regressions on Independent Slopes Model (PRISM) with a resolution of 800 m from the Climate Group at Oregon State University (Prism Climate Group, 2019).

Modern sediment samples were collected in polycarbonate tubes using a gravity corer at lake depths between 0.3 and 6 m, and the upper 1 cm of sediment was preserved for *n*-alkane analysis. We also analyzed a surface sediment sample from Libby Flats Lake, Wyoming, located within sub-alpine meadows and gymnosperm forests and which is part of a network of lakes were lake water isotopic values have been closely monitored (Liefert et al., 2018). Lake water was collected in 60 mL polypropylene bottles.

The lakes are surrounded by both tree and graminoid angiosperms, but gymnosperms trees, shrubs and forbs also grow near some of the lakes (see Supplementary Material). At each lake, leaves were sampled from the most common tree and grass species surrounding the lakes and from aquatic plants and macroalgae present in the littoral zone (at each lake, one sample per plant species, Table 2). Terrestrial leaves (2–10 leaves per individual species) were collected from trees and grasses adjacent to the lakes and tree leaves were sampled at a height of \sim 2 m above ground. Macroalgae, aquatic submergent, aquatic floating and aquatic emergent plants were collected from the littoral zone where present (2–10 leaves per aquatic plant species and 10–50 g of macroalgae). All samples were placed in Whirl-Pack bags and immediately stored at 4 °C.

Sediments and plants were freeze-dried upon arrival at the University of Wyoming. We analyzed the δ^2 H values of n-alkanes n- C_{23} to n- C_{29} in 30 surface sediment samples and in 129 plants.

2.2. Plant identification and classification

Plants were identified based on vegetative morphologies and differentiated into major taxonomic groups. Although terrestrial and aquatic plants were collected from most of the sites, here we report only the 129 plant samples for which we were able to reliably quantify n-alkane $\delta^2 H$ values. Of the 129 samples, 69 were collected from angiosperm trees, 12 from gymnosperm trees, 26 from C3 graminoids (hereafter grasses), and 21 from aquatic macrophytes. Aquatic plants were further divided into subgroups based on their growth habitat within the lake as: macroalgae (n = 4), aquatic submergent (n = 3), aquatic floating (n = 4) and aquatic emergent (n = 9).

2.3. Lake water analysis and modeled precipitation data

Lake water samples were analyzed for $\delta^2 H$ and $\delta^{18}O$ values using 12 sequential replicate measurements on a Picarro L2130 isotope analyzer at the Stable Isotope Facility at the University of

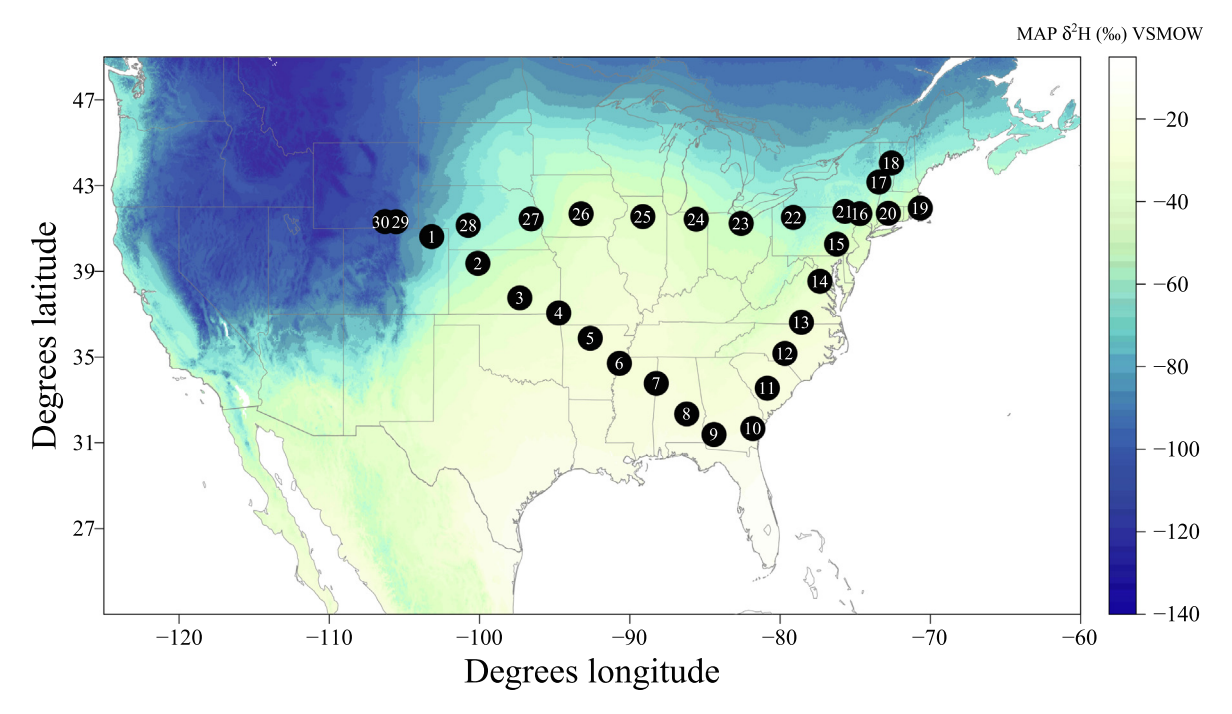


Fig. 1. Map showing the site locations for plant and surface sediment collection. Color scale displays modeled mean annual precipitation (MAP) δ²H‰ values retrieved from http://www.waterisotopes.org (Bowen, 2020). See Table 1 for sampling site information.

Table 1 Site locations, environmental data and corresponding $\delta^2 H\%$ and $\delta^{18} O\%$ values of lake water and modeled annual precipitation (MAP). $\delta^2 H\%$ and $\delta^{18} O\%$ values are reported relative to VSMOW.

Site	Latitude degrees	Longitude degrees	Elevation meters	MAT °C	MAP mm/yr	δ ² H‰ lake	δ ¹⁸ 0‰ lake	δ ² H‰ MAP	δ ¹⁸ Ο‰ ΜΑΡ
1. Overland	40.62100	-103.18200	1200	10.2	392	-90	-10.8	-73	-9.8
2. Antelope	39.37553	-100.11211	725	10.2	392	-58	-7.5	-56	-8.1
3. T1L3	37.76569	-97.31961	405	13.7	878	3	1.8	-41	-6.4
4. Spring	37.05976	-94.73146	245	14.4	1153	-9	0.2	-36	-5.9
5. Ferguson	35.88266	-92.63090	473	14.1	1175	-5	-0.2	-35	-6.1
6. Bear Creek	34.71125	-90.69264	80	16.3	1302	-16	-2.4	-29	-4.8
7. Lamar	33.77759	-88.23522	110	16.5	1431	-11	-1.4	-25	-4.6
8. T1L8	32.34999	-86.20918	87	18.2	1287	-7	-0.8	-23	-4.5
9. T1L9	31.38868	-84.39601	54	19.2	1300	14	4	-21	-3.7
10. Morgan	31.66976	-81.81111	11	19.5	1229	2	1	-21	-4
11. Turkey Hill	33.55354	-80.84634	73	17.8	1202	-28	-4.4	-26	-4.4
12. Wheatfield	35.17073	-79.67573	169	15.9	1170	-17	-2.3	-28	-4.9
13. Buffalo	36.62386	-78.57864	12	14.5	1108	-21	-2.9	-30	-5.5
14. Locust Shade	38.53797	-77.34658	45	13.6	1040	-37	-5.9	-38	-6.6
15. Middle Creek	40.27465	-76.23239	175	11.4	1139	-39	-6.1	-49	-7.9
16. T2L17	41.69247	-74.68755	479	7.7	1224	-57	-8.1	-55	-8.7
17. Carter's Pond	43.16463	-73.42084	151	7.9	1056	-56	-7.7	-60	-8.8
18. Twin Ponds	44.06117	-72.57968	410	5.5	1057	-71	-10.5	-69	-9.9
19. Arms House	41.95139	-70.66550	24	10.2	1302	-43	-6.9	-46	-7.2
20. Batterson	41.71002	-72.78982	94	10	1248	-42	-6.4	-49	-7.7
21. Blanding	41.79835	-75.67582	454	7.6	1127	-57	-8.1	-59	-9.2
22. Beaver Meadows	41.52093	-79.11079	523	7.3	1165	-59	-8.9	-65	-9.9
23. Norwalk	41.23881	-82.58788	244	9.9	966	-40	-6.2	-52	-8
24. Eagle	41.43546	-85.57648	275	9.8	954	-43	-6.6	-47	-7.1
25. Mendota	41.55853	-89.13097	235	9.5	928	-36	-5.1	-44	-6.6
26. Quarry Spring	41.68668	-93.24137	241	10.1	908	-27	-3.3	-41	-6.3
27. Cottonwood	41.44972	-96.56627	370	10.2	773	-17	-0.5	-61	-8.9
28. Cody Pond	41.15055	-100.75241	852	9.6	523	-47	-4.3	-65	-7.4
29. LaPrele Pond	41.31952	-105.54942	2181	5.4	353	-119	-14.9	-98	-13.3
30. Libby Flats	41.32491	-106.28588	3192	0.1	1014	-125	-17	-118	-16.3

Wyoming. We report the average $\delta^2 H$ (‰) and $\delta^{18}O$ (‰) values of the last 3 of the 12 replicate measurements for each lake water sample. Samples were normalized using two in-house quality assurance reference materials, which were run at the beginning, in the middle, and at the end of the analytical run. An in-house

quality control reference material was used to check the quality assurance corrections. The quality reference materials were calibrated against VSMOW and SLAP with known δ^2H isotopic values of 0% and -428%, respectively, and known $\delta^{18}O$ isotopic values of 0% and -55.5%, respectively. The standard deviation for the

Table 2Number of plant types analyzed at individual sites.

Site	Angiosperm	Gymnosperm	Grass	Algae	Submergent	Floating	Emergent	Sediment
1. Overland	1		1					1
2. Antelope	1		1				1	1
3. T1L3	2		1					1
4. Spring	1		1					1
5. Ferguson	2	1	1					1
6. Bear Creek	3		1				1	1
7. Lamar	2	1	1		2			1
8. T1L8	3		1					1
9. T1L9	2		1					1
10. Morgan	1	1	1			1	1	1
11. Turkey Hill	3	1					2	1
12. Wheatfield	1		1					1
13. Buffalo	2	1	1					1
14. Locust Shade	2	1	1					1
15. Middle Creek	6		1				1	1
16. T2L17	3		1					1
17. Carter's Pond	2	1	1		1			1
18. Twin Ponds	5	1	1	1		1		1
19. Arms House	3		1					1
20. Batterson	3						1	1
21. Blanding	3	1	1	1		1	1	1
22. Beaver Meadows	2	2	1					1
23. Norwalk	3		1					1
24. Eagle	2			1			1	1
25. Mendota	2	2	1					1
26. Quarry Spring	2							1
27. Cottonwood	3		1					1
28. Cody Pond	1		1	1				1
29. LaPrele Pond	2	1	1					1
30. Libby Flats								1

quality control reference material was 0.47‰ for $\delta^2 H$ and 0.06‰ for $\delta^{18}O$ (n=6), and the long-term averages of standard deviation for the quality control reference material are 1.06‰ for $\delta^2 H$ and 0.34‰ for $\delta^{18}O$ (n=3233).

Modeled monthly and MAP δ^2H values were obtained using the Online Isotopes of Precipitation Calculator (OIPC) (Bowen, 2020). Weighted seasonal precipitation δ^2H values were calculated as in Eq. (1) using monthly modeled OIPC δ^2H values and the PRISM long-term monthly averages of precipitation amounts (mm) for each season as follows: Winter – December, January, February (DJF); Spring – March, April, May (MAM); Summer – June, July, August (JJA); and Autumn – September, October, November (SON). Predicted δ^2H values are reported relative to VSMOW.

$$Season \ \delta^2 H(\%e) = \frac{\sum (Preciptitation_{month} \ (mm) \times \delta^2 H_{month}(\%e))}{\Sigma \ months \ (mm)} \end{(1)}$$

For comparison with our results, the global meteoric water line (GMWL, Fig. 2) was calculated as in Eq. (2) (Craig, 1961):

$$\delta^{2}H(\%_{0}) = 8 * \delta^{18}O(\%_{0}) + 10(\%_{0})$$
 (2)

2.4. n-Alkane analysis

Lipids were extracted from 2–8 g of freeze-dried sediment and 2–8 g of freeze-dried leaves using an accelerated solvent extractor (ASE Dionex 350) with dichloromethane (DCM): methanol (9:1, volume:volume, hereafter V/V). The total lipid extract was separated over aminopropyl (LC-NH2) solid phase columns using DCM: isopropanol (2:1, V/V) then re-dissolved in hexane and separated over silica gel columns using hexane to isolate the aliphatic fraction. The aliphatic fraction was re-dissolved in hexane and separated over activated 10% silver nitrate-impregnated silica gel columns to isolate the saturated n-alkane compounds.

n-Alkane δ^2 H values were measured by injecting 1 μ L of the saturated fraction into a Thermo Scientific Trace GC Ultra fitted with an Agilent DB5 column and coupled to a Thermo Delta V IRMS. The injector was held at a constant temperature of 250 °C and the reactor at a constant temperature of 1420 °C. The GC oven was held at 35 °C for 2 min then ramped 30 °C/min to a temperature of 225 °C, held for 1 min, then ramped again 10 °C/min to a final temperature of 300 °C and held for 12 min. All samples were run in duplicate. A standard n-alkane mixture (mixture A7 from Arndt Schimmelmann, Indiana University) containing n-C₁₆ to n-C₃₀ n-alkanes was used to identify the n-alkane compounds based on retention times, and to account for instrument D/H offset. The standard mixture was measured in triplicate at different concentrations $(0.05 \mu g/\mu L, 0.08 \mu g/\mu L, 0.10 \mu g/\mu L, and 0.150 \mu g/\mu L)$ at the beginning and at the end of the sequence, and the standard mixture dilutions were also analyzed in duplicate at a regular interval throughout the sequence (after every 5th sample). For each homologue, linear equations were generated using the relationships between peak area and the offset between known and measured δ^2 H values in the standard mixture, which were then applied to normalize the measured δ^2H values of individual homologues in each sample. We only report the δ^2H values of *n*-alkanes with amplitudes > 1 V. All δ^2 H measurements are reported as per mil (%) relative to the Vienna Standard Mean Ocean Water (VSMOW). The average H₃⁺ factor for all runs was 2.19 and ranged between 1.98 and 2.21 across all runs. Duplicate sample δ^2 H measurements were averaged, and the average δ^2 H difference between duplicates was 2.4% across all runs.

We only report the $\delta^2 H$ values of alkanes n- C_{23} through n- C_{29} as the concentrations of short chain n- C_{17} to n- C_{21} n-alkanes in most sediments and terrestrial plants were too low to reliably be measured for the $\delta^2 H$ isotopic composition. Similarly, we report n-alkanes $\delta^2 H$ values in aquatic plants collected from 12 of the lakes. However, aquatic plants were collected from 20 of the lake but n-alkanes concentrations were too low to be reliably quantified.

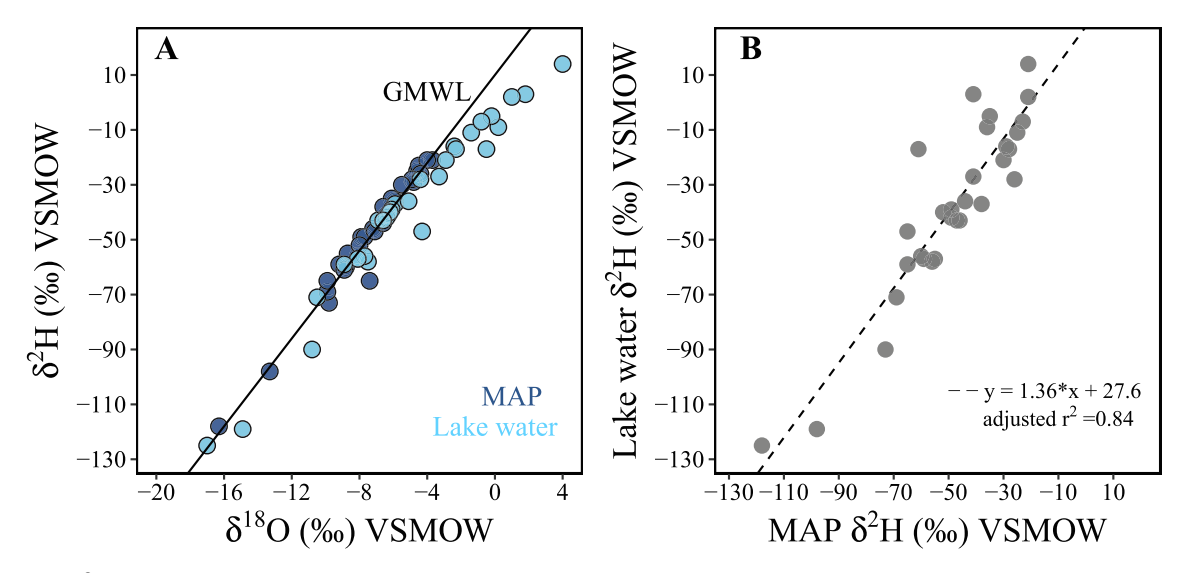


Fig. 2. A. δ^{18} O versus δ^{2} H values of measured lake water (light blue circles) show evidence of modest evaporative enrichment at some lakes compared to those of modeled mean annual precipitation (MAP, dark blue circles). Both δ^{18} O and δ^{2} H values at each of our sites are plotted with respect to the global meteoric water line (GMWL, black line). **B.** Modeled MAP versus measured lake water δ^{2} H values at each lake. (For interpretation of the references to color in this figure legend, the reader is referred to the web version of this article.)

The apparent fractionation (ε_{app}) between leaf wax n-alkanes (from sediments or plants) and source water (e.g., lake water or MAP) was calculated using Eq. (3):

$$\epsilon_{\text{wax/water}} \ (\%) = \ 1000 * \left(\frac{\delta^2 H_{\text{wax}} \ (\%) \ + \ 1000}{\delta^2 H_{\text{water}} \ (\%) \ + \ 1000} - 1 \right) \eqno(3)$$

We also applied Eq. (3) to calculate ϵ_{app} values between measured lake water and modeled MAP $\delta^2 H$ values.

We used one-way ANOVA and Tukey Honest Significant Differences tests (TukeyHSD) to check for significant differences in $\varepsilon_{\text{wax/water}}$ means between sediments and plant groups. All of our statistical treatments were completed using base functions in R (R Core Team, 2018).

3. Results

3.1. Modeled MAP and measured lake water δ^2 H values

Modeled MAP $\delta^2 H$ and $\delta^{18} O$ values at our sample sites plot along the GMWL and range from -118% to -21% and from -16.3% to -4%, respectively (Fig. 2A, Table 1). Measured lake water $\delta^2 H$ and $\delta^{18} O$ values also plot along or near the GMWL and range from -125% to 3% and from -17% to 1.8%, respectively. Overall, most of our sites cluster along the mid- to high-end range of modeled precipitation and measured lake water $\delta^2 H$ and $\delta^{18} O$ values.

Modeled MAP and measured lake water $\delta^2 H$ values are highly correlated across sites (Pearson's correlation coefficient, r=0.92, p=<0.01) (Fig. 2B), with differences between lake water and MAP $\delta^2 H$ values ($\epsilon_{lake/MAP}$) ranging from -23% to 47% (mean = 10%). Furthermore, measured lake water $\delta^2 H$ values correlate more with modeled MAP $\delta^2 H$ values (Pearson's r=0.92, p=<0.05) than with the seasonal $\delta^2 H$ values (Table 3). Consequently, we use MAP $\delta^2 H$ values as the variable of interest in our subsequent analyses. Seasonally, measured lake water $\delta^2 H$ values best correlate with the modelled $\delta^2 H$ values of MAM precipitation (Table 3, Pearson's r=0.82, p<0.05). Modeled MAP $\delta^2 H$ values also correlate best with modeled seasonal $\delta^2 H$ values of spring precipitation (Table 3, MAM: Pearson's r=0.89, p<0.05).

Table 3 Pearson correlation values between predicted MAP and predicted seasonal $\delta^2 H\%$ values and between MAP and measured lake water $\delta^2 H\%$ values (n = 30). All correlations are significant (p < 0.05).

Variable	MAP	Lake water		
DJF	0.757	0.650		
MAM	0.887	0.817		
JJA	0.885	0.814		
SON	0.855	0.745		

3.2. $\varepsilon_{alkane/MAP}$ values across plant groups and sediments

We calculated $\varepsilon_{\rm alkane/MAP}$ values for surface sediments and for individual plant groups (Fig. 3; Table 4). $\varepsilon_{\rm alkane/MAP}$ values for n- C_{23} to n- C_{29} in sediments and individual plant groups vary, but estimates based on n-alkanes from sediment and terrestrial plants overlap (Fig. 3; Table 4). For both mid- and long-chain n-alkanes, $\varepsilon_{\rm alkane/MAP}$ distributions are similar for sediments and angiosperm plants; the means fall within 1‰, 6‰, 0‰, and 4‰ for n- C_{29} , n- C_{27} , n- C_{25} and n- C_{23} , respectively (Fig. 3). Gymnosperm $\varepsilon_{\rm alkane/MAP}$ distributions are similar to those of sediments for n- C_{29} and n- C_{29} (within 1‰ and 5‰, respectively), but lower than those of sediments for n- C_{27} and n- C_{25} (by 13‰).

Mean $\varepsilon_{\rm alkane/MAP}$ values for grasses, however, are consistently lower than for sediments (by >15%; Fig. 3). Mean $\varepsilon_{\rm alkane/MAP}$ is also lower for all aquatic plant groups than for sediments (by 16–51%) with most of aquatic $\varepsilon_{\rm alkane/MAP}$ distributions plotting below the means of $\varepsilon_{\rm alkane/MAP}$ in sediments (Fig. 3). Even though the water source of aquatic plants is lake water, mean $\varepsilon_{\rm alkane/lake}$ values for aquatic plant n-alkanes versus lake water are also consistently lower (by >24%) than those of sediments (Table 4). Due to low abundances of n-C₂₃ and n-C₂₅ in floating plants, we were unable to reliably calculate their $\varepsilon_{\rm alkane/MAP}$ distributions.

A one-way ANOVA test revealed no significant differences in $\epsilon_{alkane/MAP}$ means between aquatic plant groups (Pr(>F) > 0.05), therefore, we combined all aquatic plants and plotted their $\epsilon_{alkane/MAP}$ distribution in each panel in Fig. 3 (light blue). With the $\epsilon_{alkane/MAP}$ distributions incorporating all the aquatic plants, a one-way ANOVA test revealed significant differences (Pr(>F) < 0.0 5) in $\epsilon_{alkane/MAP}$ means between sediments and different

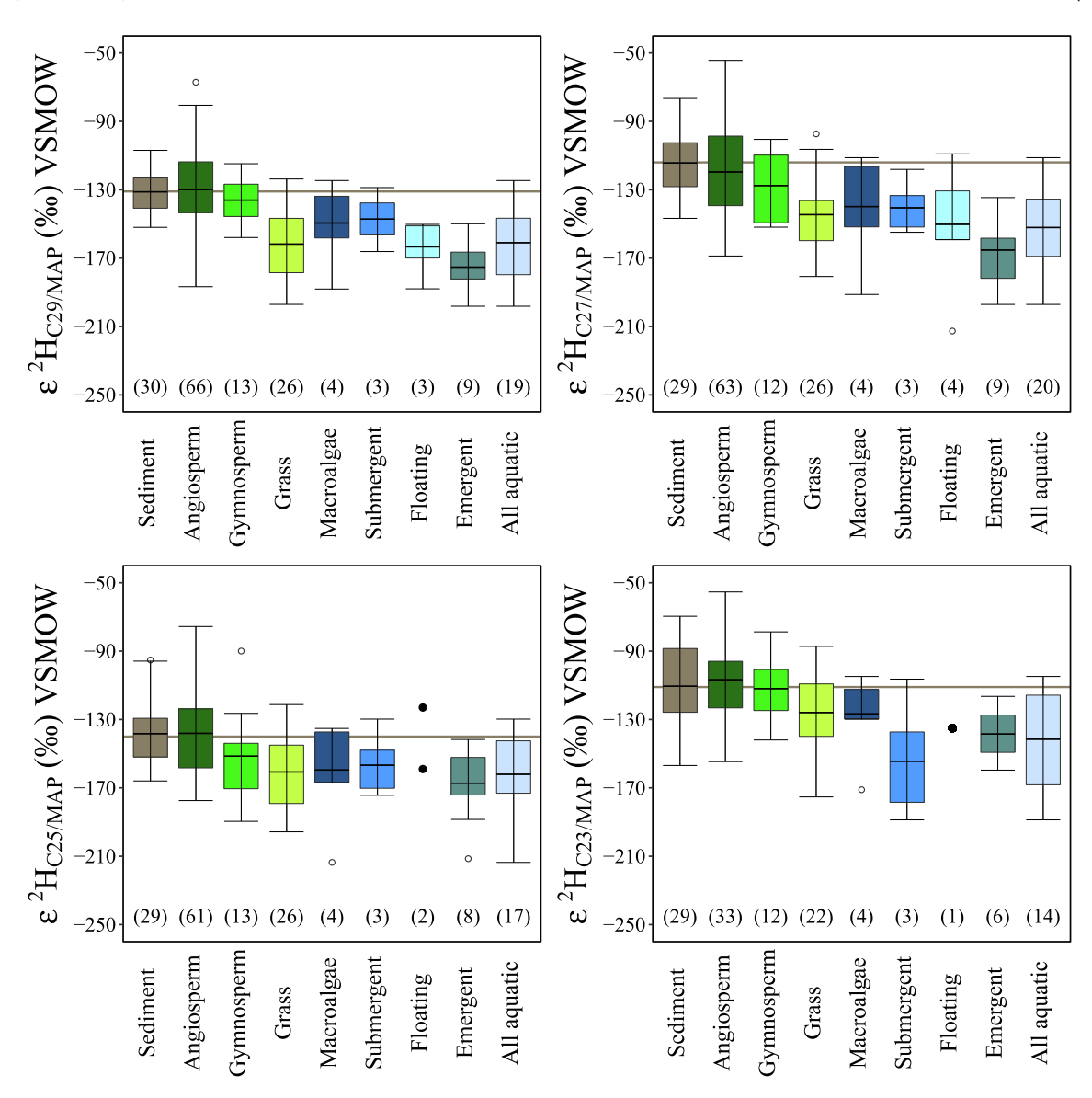


Fig. 3. Distributions of the apparent fractionation (ε_{app}) between n-alkanes and MAP $\delta^2H\%$ values for sediments and different plant groups for n- C_{23} to n- C_{29} (odd alkanes). Horizontal lines represent the mean ε_{app} value between sediments and MAP ($\varepsilon_{sediment/MAP}$) for each n-alkane and the sample size for each distribution is shown in parentheses. Boxplot statistics are as follows: lower whisker = lowest value, lower hinge = first quantile, middle hinge = mean, upper hinge = third quantile, and upper whisker = highest value. Open circles represent outlier data and black filled circles represent actual data points.

plant groups for n- C_{23} , n- C_{25} , n- C_{27} , and n- C_{29} . Therefore, we used a TuckyHSD test to identify the groups with significant differences in $\epsilon_{alkane/MAP}$ means. The TuckyHSD test identified significant differences (adjusted p < 0.05) in $\varepsilon_{\text{alkane/MAP}}$ means between those of all aquatic plants (Fig. 3, light blue boxplots) and those of sediments and angiosperm for n- C_{23} , n- C_{25} , n- C_{27} and n- C_{29} . Except for n-C₂₅, the all aquatic plants $\epsilon_{alkane/MAP}$ means are also significantly different than those of gymnosperm. Grass $\epsilon_{alkane/MAP}$ means are significantly different than those of sediments for $n-C_{25}$, n- C_{27} and n- C_{29} , than those of angiosperm for n- C_{23} , n- C_{25} , n- C_{27} and n- C_{29} , and than those of gymnosperm for n- C_{29} (adjusted p < 0.05). We found no significant differences (adjusted p > 0.05) between the $\varepsilon_{alkane/MAP}$ means of all aquatic plants (Fig. 3, light blue boxplots) and those of grasses, between those of angiosperm and gymnosperm plants, between those of sediments and angiosperm plants, or between those of sediments and gymnosperm plants.

3.3. Sources of n- C_{23} and n- C_{29} in lake sediments

Differences in $\delta^2 H$ values between $n\text{-}C_{29}$ and $n\text{-}C_{23}$, represented by $\epsilon_{\text{C29/C23}}$ values, differ among sources (Fig. 5). Comparisons with $\epsilon_{\text{C29/C23}}$ based on n-alkanes from different plant sources highlight similarities in the isotopic composition of sediments and terrestrial plants. At our sites, the $\epsilon_{\text{C29/C23}}$ distributions reveal that $n\text{-}C_{29}$ $\delta^2 H$ values in sediments averaged $\sim 22\%$ lower than those of $n\text{-}C_{23}$ (s.d. = 24%; Fig. 5). The sediment $\epsilon_{\text{C29/C23}}$ distribution is similar to that of angiosperm trees (mean = -18%, s.d. = 26%), gymnosperm trees (mean = -26%, s.d. = 16%), and grasses (mean = -38%, s.d. = 23%). We find no significant differences in $\epsilon_{\text{C29/C23}}$ means between sediments, angiosperm, gymnosperm, grasses and submergent aquatic plants (TukeyDSD adjusted p > 0.05), although, submerged aquatic plants, often assumed to be a major source of $n\text{-}C_{23}$, represent an extreme difference with a positive $\epsilon_{\text{C29/C23}}$ mean (mean = 10%, s.d. = 38%).

Table 4
Apparent fractionation factors between *n*-alkanes δ^2 H‰ values and modeled annual precipitation and lake water δ^2 H‰ values in sediments and different plant types (ε_{wax/MAP}, ε_{wax/lake}).

Туре	$arepsilon_{ ext{wax/MAP}}$				$\epsilon_{ m wax/lake}$			
	C29	C27	C25	C23	C29	C27	C25	C23
Sediment	-131 ± 12‰	-114 ± 17‰	-138 ± 20‰	-111 ± 24‰	-140 ± 18‰	-123 ± 19‰	-147 ± 21‰	-119 ± 24‰
	n = 30	n = 29	n = 29	n = 29	n = 30	n = 29	n = 29	n = 29
Angiosperm	$-130 \pm 21\%$	$-120 \pm 24\%$	-138 ± 23‰	$-107 \pm 24\%$	_	_	_	_
	n = 66	n = 63	n = 61	n = 32				
Gymnosperm	$-136 \pm 14\%$	$-128 \pm 21\%$	$-151 \pm 27\%$	-112 ± 21‰	_	_	_	_
-	n = 13	n = 12	n = 13	n = 12				
Grass	$-162 \pm 23\%$	$-145 \pm 22\%$	$-161 \pm 23\%$	$-126 \pm 22\%$	_	_	_	_
	n = 26	n = 26	n = 26	n = 22				
Algae	$-149 \pm 28\%$	$-140 \pm 36\%$	$-160 \pm 37\%$	$-127 \pm 30\%$	-163 ± 19‰	$-154 \pm 29\%$	$-173 \pm 30\%$	$-140 \pm 28\%$
_	n = 4	n = 4	n = 4	n = 4	n = 4	n = 4	n = 4	n = 4
Submergent	$-147 \pm 19\%$	$-141 \pm 20\%$	$-157 \pm 24\%$	$-154 \pm 43\%$	$-156 \pm 23\%$	$-150 \pm 24\%$	$-166 \pm 28\%$	$-164 \pm 47\%$
	n = 3	n = 3	n = 3	n = 3	n = 3	n = 3	n = 3	n = 3
Floating	$-163 \pm 21\%$	$-150 \pm 44\%$	$-141 \pm 26\%$	-135%	$-163 \pm 20\%$	$-154 \pm 43\%$	$-141 \pm 29\%$	$-137\%_{o}$
	n = 3	n = 4	n = 2	n = 1	n = 3	n = 4	n = 2	n = 1
Emergent	$-175 \pm 15\%$	$-165 \pm 21\%$	$-167 \pm 23\%$	-139 ± 16‰	−179 ± 15‰	$-169 \pm 23\%$	$-171 \pm 30\%$	$-140 \pm 19\%$
	n = 9	n = 9	n = 8	n = 6	n = 9	n = 9	n = 8	n = 6
All aquatic	$-161 \pm 22\%$	$-152 \pm 26\%$	$-162 \pm 25\%$	-141 ± 30%	$-169 \pm 20\%$	$-160 \pm 25\%$	$-170 \pm 27\%$	$-149 \pm 32\%$
=	n = 19	n = 20	n = 17	n = 14	n = 14	n = 14	n = 14	n = 14

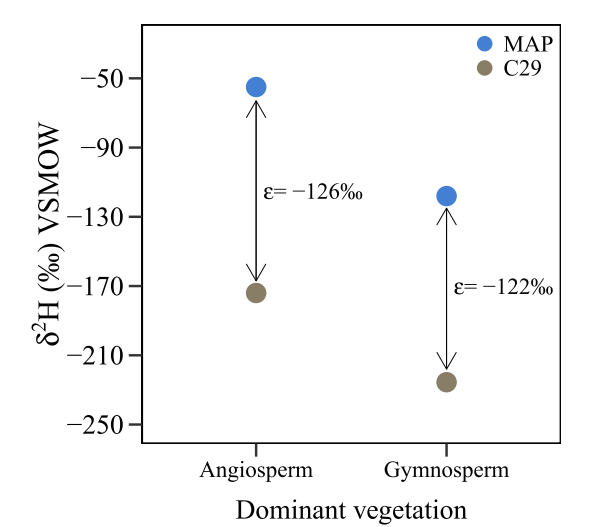


Fig. 4. ε_{app} values (arrows) between n- C_{29} (tan points) and MAP (blue points) $\delta^2 H$ values are similar at an angiosperm tree dominated site versus a gymnosperm tree dominated site. (For interpretation of the references to color in this figure legend, the reader is referred to the web version of this article.)

Assuming a constant angiosperm source of $n\text{-}C_{29}$ in sediments, but different plant sources of $n\text{-}C_{23}$, produces a range of different outcomes (Fig. 5, white boxplots). We find that the $\epsilon_{\text{C29angiosperm/C23submergent}}$ mean (mean = 34%, s.d. = 31%) is significantly different than $\epsilon_{\text{C29/C23}}$ means in sediments, angiosperm, gymnosperm, grasses, angiosperm/gymnosperm, and angiosperm/grass (TukeyHSD adjusted p < 0.05). Submergent aquatic plant sources of $n\text{-}C_{23}$ produced positive $\epsilon_{\text{C29/C23}}$ values, suggesting that $n\text{-}C_{29}$ $\delta^2\text{H}$ values in angiosperm plants are consistently more positive (by $\sim 56\%$) than $n\text{-}C_{23}$ $\delta^2\text{H}$ values in submerged aquatic plants. We also find significant differences between the $\epsilon_{\text{C29/C23}}$ means in angiosperm/grass (mean = -3.4, s.d. = 29%) and those of sediments, grasses, and angiosperm/ submergent as well as between the $\epsilon_{\text{C29/C23}}$ means in angiosperm/gymnosperm (mean = -13%, s.d. = 23%) and grasses.

3.4. Comparison with global sedimentary wax δ^2 H values

The δ^2 H values of MAP, lake water, sedimentary n- C_{23} and n- C_{29} (Fig. 6, red points) plot consistently along with other global δ^2 H

datasets compiled by McFarlin et al. (2019) with additional data from Ladd et al. (2021) (Fig. 6, grey and blue points). Our 30 new measurements of n-C₂₉ δ^2 H values from surface sediments do not depart from the global relationship with MAP δ^2 H values (Fig. 6A). Adding our data, updates the global relationship to

$$n-C_{29} \delta^2 H(\%_0) = 0.76 \times (MAP \delta^2 H(\%_0)) - 132,$$

and slightly improves the coefficient of determination (r^2) from 0.83 to 0.84; McFarlin et al. (2019) found that

$$n-C_{29} \delta^2 H(\%) = 0.78 \times (MAP \delta^2 H(\%)) - 129.$$

We also find that, at a global scale, n- C_{29} $\delta^2 H$ values from sediments are significantly correlated to lake water $\delta^2 H$ values (r^2 = 0.64, p < 0.01) (Fig. 6B). Although there is more scatter in the relationship between n- C_{29} $\delta^2 H$ values and those of lake water than with those of MAP, the scatter clusters around sites from high latitudes (>65°N) where lake water $\delta^2 H$ values can be decoupled from MAP $\delta^2 H$ values (Cluett and Thomas, 2020; Thomas et al., 2020).

In the case of the n-C₂₃-alkane (Fig. 6C and D), our additional δ^2 H measurements also improve the global relationships with both MAP and lake water δ^2 H values (r^2 = 0.52 and 0.63, respectively, compared to r^2 = 0.3 and 0.4, respectively, from McFarlin et al., 2019). Importantly, however, the slopes of the updated global relationships for MAP and lake water do not differ, within uncertainty error, from each other or from the n-C₂₉ relationships: 0.76 (s. e. = 0.08) for MAP and 0.73 (s.e. = 0.07) for lake water (Fig. 6C and D).

Using the linear relationships between MAP and n- C_{29} $\delta^2 H$ values and between lake water and n- C_{23} $\delta^2 H$ values from Fig. 6A and C to predict MAP and lake water $\delta^2 H$ values, respectively (Fig. 7A), we find no significant differences in the slopes, within uncertainty error: 1.00 (s.e. = 0.10) for MAP and 0.99 (s.e. = 0.10) for lake water (Fig. 7A). Instead, the overlap between predicted MAP and predicted lake water $\delta^2 H$ values is consistent with the similar correlations of $\delta^2 H$ values among MAP, lake water, and both n- C_{29} and n- C_{23} (Fig. 6). We detect a significant correlation (p < 0.05) between n- C_{23} and n- C_{29} $\delta^2 H$ values (Fig. 7E). n- C_{25} and n- C_{27} $\delta^2 H$ values in sediments also correlate significantly with n- C_{29} $\delta^2 H$ values at a global scale (p < 0.05), and global correlations intercepts (Fig. 7C-E) agree with the terrestrial plants ϵ_{app} means calculated for our sites (Fig. 3).

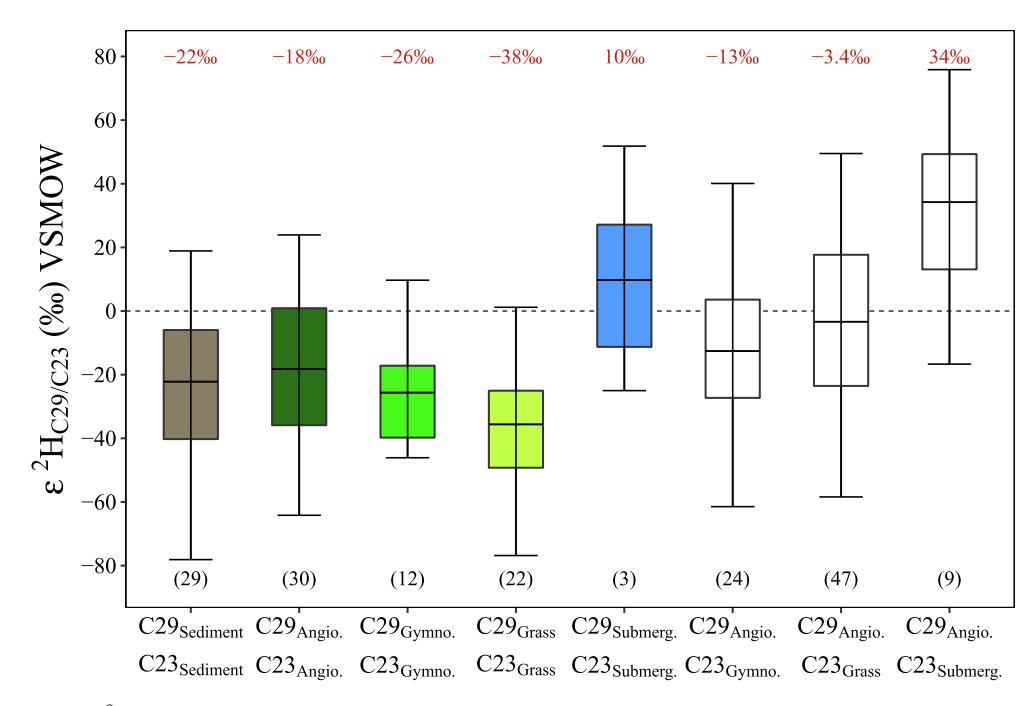


Fig. 5. Distributions showing the δ^2 H‰ differences ($\varepsilon_{C29/C23}$) between n- C_{29} and n- C_{23} in sediments and within plant groups (colored boxplots) and between a constant n- C_{29} angiosperm source and varying n- C_{23} sources (white boxplots). Horizontal dashed line is plotted at $\varepsilon_{C29/C23} = 0$ ‰. Boxplot statistics are as follows: lower whisker = lowest value, lower hinge = first quantile, middle hinge = mean, upper hinge = third quantile and upper whisker = highest value.

In parallel, we find no significant correlation (p > 0.05) between the n-C₂₉ and n-C₂₃ δ^2 H difference ($\varepsilon_{C29/C23}$) in the global sediments and the Lake/MAP δ^2 H difference ($\varepsilon_{Lake/MAP}$) related to evaporation (Fig. 7B). We find that the $\epsilon_{\text{C29/C23}}$ mean in global sediments (-11‰, Fig. 7B, grey boxplot) is not statistically different than the $\varepsilon_{C29/C23}$ mean in angiosperm plants (TukeyHSD adjusted p > 0.05; Fig. 7B, dark green boxplot). Conversely, the $\varepsilon_{C29/C23}$ mean in global sediments is significantly different than the $\epsilon_{C29/C23}$ mean of mixed angiosperm and aquatic submergent plants input (TukeyHSD adjusted p < 0.05; Fig. 7B, white boxplot). Some of the data might represent aquatically-derived n- C_{23} (i.e., samples with high $\varepsilon_{C29/C23}$ values overlapping with the $\varepsilon_{C29/C23}$ range expected by mixing submerged and terrestrial sources, white boxplot, Fig. 7B), but the global dataset supports a dominantly terrestrial source of sedimentary n- C_{23} . Most $\varepsilon_{C29/C23}$ values in the global sediment dataset (89%) lie below the mean of $\varepsilon_{angiospermC29/submergedC23}$ (gray boxplot, Fig. 7B), and 84% fall within the $\epsilon_{angiospermC29/angiospermC23}$ distribution (dark green boxplot, Fig. 7B).

4. Discussion

4.1. Provenance of mid- and long-chain n-alkanes in sedimentary archives

Previous studies show that submerged and floating aquatic plants favor the production of mid-chain n-alkanes (Aichner et al., 2010a; Ficken et al., 2000; Nichols et al., 2006; Gao et al., 2011). Therefore, the sedimentary n- C_{23} -alkane has been interpreted as being derived from aquatic submerged plants (Ficken et al., 2000; Seki et al., 2011; Rach et al., 2014; Rach et al., 2017; Curtin et al., 2019; Puleo et al., 2020). Here, we show that n-alkanes δ^2 H values in plants and lake sediments from across North America do not support such an inference. Instead, the δ^2 H values in plants and sediments at our sites suggest a terrestrial source of mid-chain n-alkanes in sedimentary archives (Figs. 3 and 5).

The distributions of ε_{app} values support a dominantly angiosperm tree source of mid- and long-chain n-alkanes in sediments where mean $\epsilon_{\text{wax/MAP}}$ values for angiosperm trees are not significantly different than those of sediments (TukeyHSD adjusted p > 0.05, Fig. 3). Conversely, mean $\varepsilon_{\text{C23/MAP}}$ and $\varepsilon_{\text{C29/MAP}}$ values for grasses and aquatic plants are significantly lower than those of sediments (by >15%; TukeyHSD adjusted p < 0.05). Moreover, mean $\varepsilon_{\text{C23/MAP}}$ and $\varepsilon_{\text{C29/MAP}}$ in aquatic plants are also significantly different than those of sediments, angiosperm plants, and gymnosperm plants (by >25%; TukeyHSD adjusted p < 0.05). Differences in ϵ_{app} means between aquatic plants and sediments, or angiosperm and gymnosperm trees are slightly larger if we consider the ϵ_{app} between \emph{n} -alkanes and lake water for sediments and aquatic plants (Table 4). The lower ϵ_{app} values in aquatic plants compared to angiosperms and gymnosperms is consistent with previous findings (Chikaraishi and Naraoka, 2003; Duan et al., 2014; Aichner et al., 2017; Dion-Kirschner et al., 2020). Mosses are another possible contributor to the sedimentary n-C₂₃ pool as they have been shown to primarily synthesize mid-chain n-alkanes (Sachse et al., 2006; Nichols et al., 2009; Bush and McInerney, 2013; Hollister et al., 2022). Although we did not sample mosses in this study, moss $\varepsilon_{\text{C39/MAP}}$ values have been shown to be more positive than those of terrestrial plants (Sachse et al., 2006). Therefore, if mosses were a major contributor of n-C₂₃-alkane in sediments at our sites, sediment $\varepsilon_{\text{C23/MAP}}$ values would have been more positive than those of terrestrial plants (Fig. 3).

Our results challenge the assumption that submerged aquatic plants produce the n- C_{23} -alkane incorporated in sediments, which has led to the use of $\varepsilon_{C29/C23}$ as a proxy for terrestrial evapotranspiration (i.e., $\varepsilon_{terr-aquatic}$; Seki et al., 2011; Rach et al., 2014, Rach et al., 2017; Curtin et al., 2019). The rationale behind this assumption is that long-chain n-alkanes in terrestrial plants (e.g., n- C_{29}) track MAP δ^2 H values plus an additional enrichment from soil and leaf water evaporation (Sachse et al., 2004). If lake water can be assumed to have experienced little evaporative enrichment, then the n- C_{23} -alkane in submergent aquatic plants should track

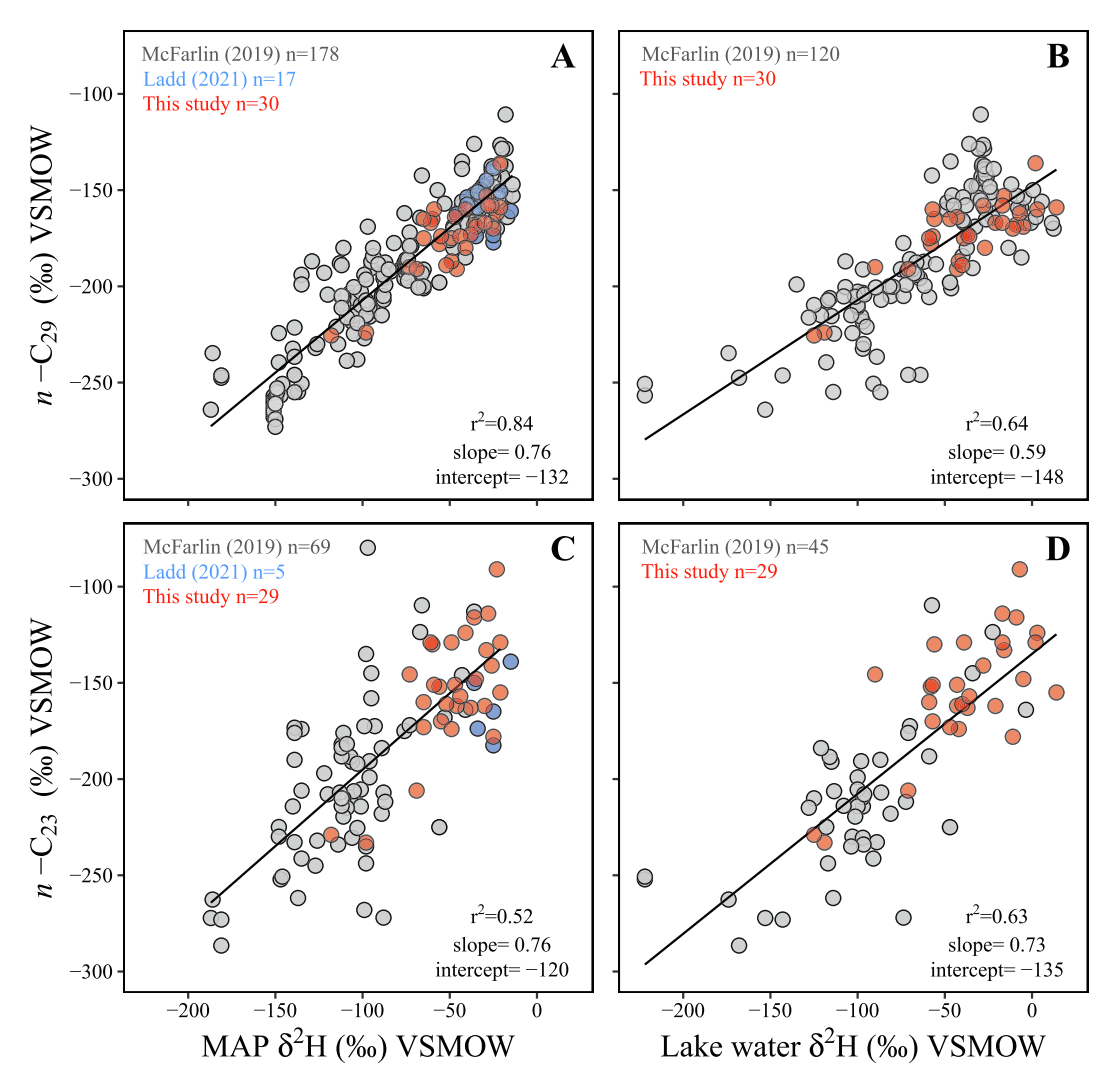


Fig. 6. Scatterplots showing the global relationships between modeled MAP and measured lake water $\delta^2 H\%$ values versus n-C₂₉ and n-C₂₃ $\delta^2 H\%$ values in global sediments. Compiled global $\delta^2 H\%$ data for lake water, modeled MAP, n-C₂₉ and n-C₂₃ were obtained from McFarlin et al. (2019) and Ladd et al. (2021) and are shown with gray and blue points respectively; this study $\delta^2 H\%$ data are shown with red points. All the relationships are statistically significant (p < 0.05). (For interpretation of the references to color in this figure legend, the reader is referred to the web version of this article.)

the original MAP δ^2 H values; if not, $n\text{-}C_{23}$ could record the δ^2 H signature of amplified evaporation within a lake. Either way, the $\epsilon_{\text{C29/C23}}$ values would reflect the strength of either soil or lake evaporation depending upon the sign of the difference. Such a range of outcomes could be supported given that the mean ϵ_{app} between n-C₂₉ δ^2 H values and n-C₂₃ δ^2 H values in sediments is –22‰ with a large standard deviation of 24‰ (Fig. 5).

However, ε_{app} values vary between individual n-alkanes and within individual plant groups (Fig. 3), and $\varepsilon_{C29/C23}$ values in sediments are similar to those observed in angiosperm and gymnosperm trees (Fig. 5). Moreover, if submerged aquatic plants would be the dominant source of n- C_{23} and higher terrestrial plants the dominant source of n- C_{29} (e.g., angiosperms) in sediments at our sites, then the mean values of $\varepsilon_{C29/C23}$ in sediments would be positive (mean ε angiosperm $\varepsilon_{C29/Submerged}$ = 34%; Fig. 5). Instead, the observed offsets in most sediments appear because n- ε_{C23} ε_{C23} values are more positive than ε_{C29} $\varepsilon_{C29/C23}$ signifies variations in ε_{app} between ε_{C23} and ε_{C29} $\varepsilon_{C29/C23}$ signifies variations in ε_{app} between ε_{C23} and ε_{C29} $\varepsilon_{C29/C23}$ signifies variations in ε_{app} between ε_{C23} and ε_{C29} $\varepsilon_{C29/C23}$ signifies variations in ε_{app} between ε_{C23} and ε_{C29} $\varepsilon_{C29/C23}$ signifies variations in ε_{app} between ε_{C23} and ε_{C29} $\varepsilon_{C29/C23}$ signifies variations in ε_{app} between ε_{C23} and $\varepsilon_{C29/C23}$ signifies variations in $\varepsilon_{C29/C23}$ signifies variati

The dominance of terrestrial angiosperm trees as the source of mid- and long-chain n-alkanes in lake sediments could be explained by differences in: (1) aquatic versus terrestrial tree distributions in and around lakes, and (2) the rate of *n*-alkane production in aquatic versus terrestrial plants (Dion-Kirschner et al., 2020). In general, the distribution of submerged aquatic plants is limited to the aquatic near-shore zone of lakes where photosynthesis can occur (Jiang et al., 2021). Conversely, terrestrial plants extend over large water- and air-sheds around most lakes and previous studies show that regionally sourced leaf wax aerosols (from tens to hundreds of km away) are also an important contributor to lake sediments (Gao et al., 2014; Nelson et al., 2018). Additionally, previous studies show that aquatic plants produce 30x less leaf wax while shoreline plants produce 10-300x less leaf wax than terrestrial plants per unit of leaf biomass ($\mu g/g$; Freimuth et al., 2019; Dion-Kirschner et al., 2020). Consequently, greater rates of nalkane production on terrestrial tree leaves and the larger extent of terrestrial ecosystems combine to favor angiosperm tree leaf wax contribution to the sediments, masking the weak signal of mid-chain n-alkanes produced by aquatic plants. Even though terrestrial plants synthesize less mid-chain than long-chain n-alkanes

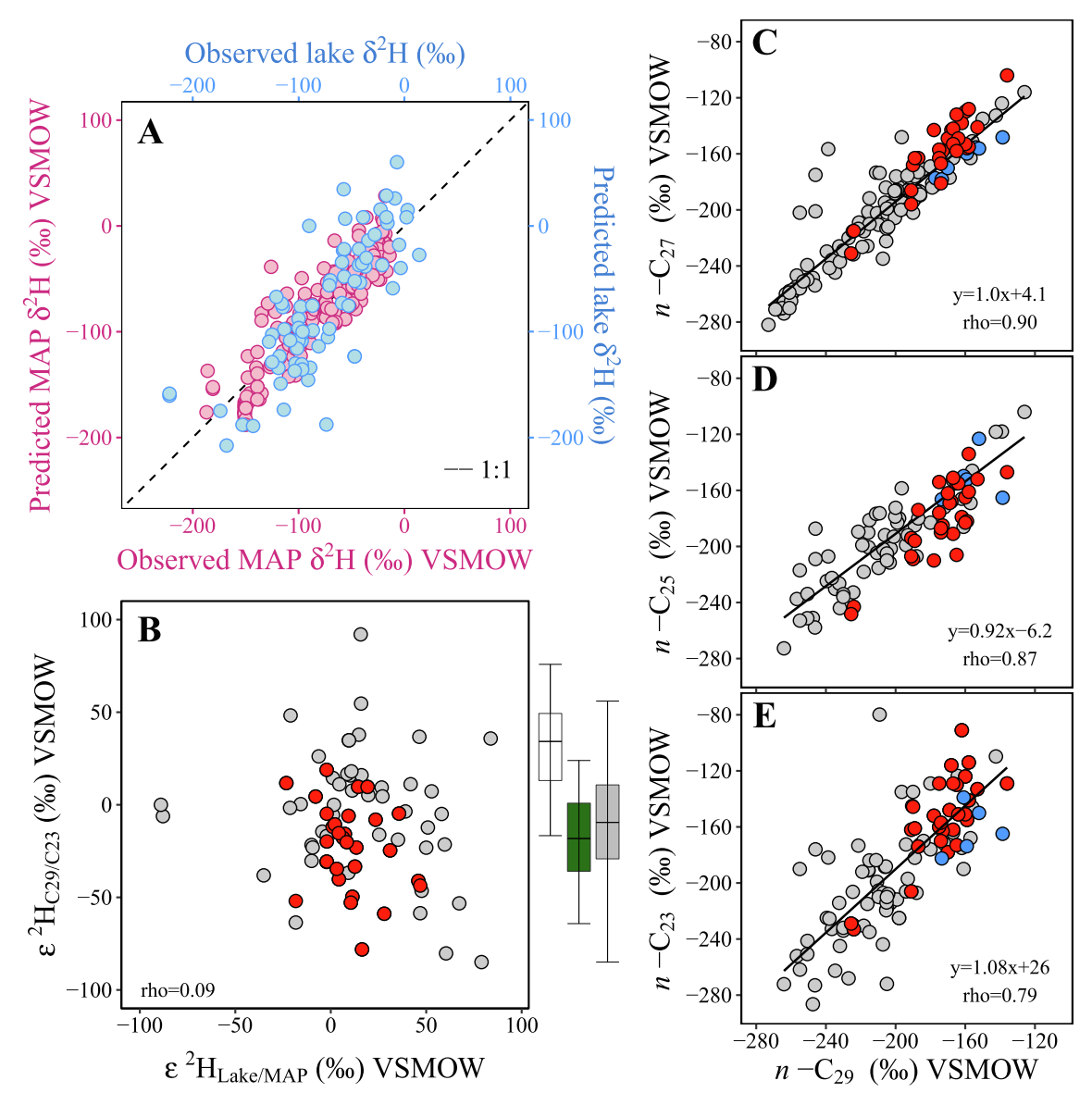


Fig. 7. A. Scatterplot showing the observed versus predicted MAP δ^2 H‰ values (red points, n=208) calculated based on the n-C₂₉ δ^2 H‰ relationship to MAP δ^2 H‰ shown in Fig. 6A, and the observed versus predicted lake water δ^2 H‰ values (blue points, n=74) based on the n-C₂₃ δ^2 H‰ relationship to lake water δ^2 H‰ shown in Fig. 6D; the 1:1 line is shown in black. **B.** ε_{app} values between modeled MAP and measured lake water (ε_{MAP/lake}) versus ε_{app} values between sediment n-C₂₉ and n-C₂₃ (ε_{C29/C23}) (n=74); boxplots show the distribution of ε_{C29angiosperm/(C23angiosperm/(C23angiosperm/(C23angiosperm)} (and the distribution of ε_{C29l/C23} in global sediments (grey). Boxplot statistics are as follows: lower whisker = lowest value, lower hinge = first quantile, middle hinge = mean, upper hinge = third quantile, and upper whisker = highest value. **C-E.** Scatterplots showing the global relationship between sedimentary n-C₂₉ and n-C₂₇ δ^2 H‰ (n=115); n-C₂₉ and n-C₂₅ δ^2 H‰ (n=58); and n-C₂₉ and n-C₂₃ δ^2 H‰ (n=95) with linear regression and Spearman's rho values shown in each plot. Data from this study is shown with red points, from the global dataset compiled by McFarlin et al. (2019) is shown with grey points, and from Ladd et al. (2021) is shown with dark blue points. (For interpretation of the references to color in this figure legend, the reader is referred to the web version of this article.)

(Ficken et al., 2000; Gao et al., 2011), terrestrial trees act as the dominant sources for both chain lengths (Diefendorf and Freimuth, 2017). Therefore, we recommend the use of other lake water isotopic proxies such as short-chain *n*-alkanes and *n*-alkanoic acids that are primarily synthesized by algae (Huang et al., 2002; Sachse et al., 2012).

4.2. ε_{app} as a function of vegetation type

In our dataset, ε_{app} varies within and between individual plant groups and, therefore, individual plant groups have different influences on the ε_{app} values of n-alkanes deposited in sedimentary archives (Fig. 3, Table 4). Thus, information on the vegetation contributing to the sedimentary n-alkane pool is crucial for inferring

source water δ^2 H values. Below we discuss the impact of vegetation changes on n- C_{29} , as n- C_{29} is the most abundant n-alkane in sediments and most commonly used for inferring the δ^2 H values of precipitation.

Across different regions, and through time, vegetation changes might affect $n\text{-}C_{29}$ $\delta^2\text{H}$ values preserved in lake sediments due to differences in $\epsilon_{\text{C29/MAP}}$ values between different plant groups. Consistent with previous findings (Chikaraishi and Naraoka, 2003), we find no significant difference in $\epsilon_{\text{C29/MAP}}$ means between angiosperm and gymnosperm trees (Fig. 3, Table 4) suggesting that vegetation shifts between angiosperms and gymnosperms trees would not impact $n\text{-}C_{29}$ $\delta^2\text{H}$ signatures in sedimentary archives. These results are reinforced when comparing $\epsilon_{\text{C29/MAP}}$ values in lake sediments collected from an angiosperm tree dominated site (Lake

#16) and a gymnosperm tree dominated site (Lake #30) (Figs. 1 and 4). At these sites, $\varepsilon_{C29/MAP}$ values in lake sediments are similar (Fig. 4): $\varepsilon_{C29/MAP}$ of -126% and -122% ($\pm 2.4\%$) for the angiosperm and gymnosperm dominated sites, respectively, and both $\varepsilon_{\rm C29/MAP}$ values fall within the range of reported global sedimentary $\varepsilon_{C29/MAP}$ values of $-121\pm18\%$ (McFarlin et al., 2019). The similar $\epsilon_{\text{C29/MAP}}$ values at our two most extremely different angiosperm and gymnosperm sites (Fig. 4) demonstrate that sedimentary $n-C_{29}$ δ^2H values should track the δ^2H values of source water with a relatively constant ε_{app} even if shifts in vegetation sources do occur (i.e., angiosperm trees to gymnosperm trees, or vice versa). Nevertheless, while $\epsilon_{\text{C29/MAP}}$ values in angiosperm and gymnosperm trees do appear to be similar across North American tree species, the similarity in $\epsilon_{\text{C29/MAP}}$ values needs to be further tested in angiosperm and gymnosperm species from other parts of the world (Diefendorf et al., 2015).

Grasses may present a challenge, however. The mean $\varepsilon_{\text{C29/MAP}}$ value in grasses is significantly different than the means of angiosperm or gymnosperm trees, and a change from either source to grasses (or vice versa) would produce a significant shift in the δ^2 H values of sedimentary n-C₂₉. Our data support previous findings (Sachse et al., 2012; Bush and McInerney, 2013; Wang et al., 2018) and show that the grass $\varepsilon_{C29/MAP}$ mean (-162%) is significantly different (adjusted p < 0.05) than the mean in angiosperm (-130%) and in gymnosperm (-136%) (Fig. 3). A shift favoring grass inputs to sediments would decrease n- C_{29} δ^2H values by \sim 29‰, but varying *n*-alkane contributions from grasses and tress to sedimentary archives would also modify $\epsilon_{\text{C29/MAP}}$ values. Varying grass n-alkane inputs might also help explain the scatter in the global relationship between n- C_{29} and MAP δ^2 H values (Fig. 6A). Therefore, constraints on grass-derived *n*-alkane inputs should be evaluated. Previous efforts to distinguish between trees and grass inputs using the ratio between the abundance of $n-C_{31}$ and n-C₂₉ have been unsuccessful because this ratio is highly variable in both grasses and higher terrestrial plants (Bush and McInerney, 2013). Methods using δ^{13} C values can successfully distinguish between C4 and C3 plants (Tierney et al., 2017; Bhattacharya et al., 2018), but this tool does not apply well to temperate grasslands dominated by C3 plants. However, in such regions, other paleovegetation proxies such as fossil pollen abundances can help distinguish between dominant terrestrial vegetation sources (Overpeck et al., 1985).

Submerged and floating aquatic plants may also represent an important lipid source that would affect the δ^2 H values of both n-C₂₉ and n-C₂₃ in sediments (Figs. 3 and 5). Our data suggest that $\epsilon_{\text{alkane/MAP}}$ values are $\sim 17\%$ and $\sim 43\%$ more negative in submerged aquatic plants than in angiosperms for n- C_{29} and n- C_{23} , respectively (Fig. 3). Therefore, $\varepsilon_{C29/C23}$ may help to distinguish between submerged aquatic plant and angiosperm inputs (Fig. 5). Our results show that n- C_{23} δ^2H values are more positive than n-C₂₉ δ²H values in angiosperm trees, gymnosperm trees, and grasses, while $n-C_{23}$ δ^2H values are more negative than $n-C_{29}$ δ^2H values in submerged aquatic plants. However, given that aquatic plants produce much less leaf waxes per unit of mass compared to terrestrial plants (Freimuth et al., 2019; Dion-Kirschner et al., 2020), a dominant submerged aquatic source of n-C29-alkane is unlikely, except in the absence of higher terrestrial plants around the lakes, as is the case with desert lakes (Wang et al., 2018).

Submerged and floating aquatic plants may, conversely, represent an important source of n- C_{23} alkane (Ficken et al., 2000, Puleo et al., 2020), but that does not appear to be the case at most of our sites. Higher terrestrial plants produce most of the n- C_{23} -alkane based on isotopic compositions (Fig. 3) and $\varepsilon_{C29/C23}$ distributions (Fig. 5). If the sedimentary n- C_{23} source is aquatic submergent plants, the $\varepsilon_{C29angiosperm/C23submerged}$ distribution should be \sim 52% more positive than sediments with a higher terrestrial plant

source (mean $\epsilon_{C29angiosperm/C23submerged} = 34\%$). Consequently, $\epsilon_{C29/C23}$ values in sediments equal or greater than the mean of $\epsilon_{C29angiosperm/C23submerged}$ from our study sites (mean = 34%) are indicative of aquatic submerged plant input and, therefore, n- C_{23} δ^2 H values can be used as proxy for lake-water δ^2 H values in those cases

Nevertheless, previous studies show that changes in $\varepsilon_{C29/C23}$ values in sedimentary records can be consistent with other paleoclimate proxies of evapotranspiration at sites where a predominant aquatic source for n- C_{23} -alkane can be constrained (Rach et al., 2014; Curtin et al., 2019). However, our data shows that without a predominant aquatic input constrain on the n-C23-alkane in sedimentary archives, $\epsilon_{\text{C29/C23}}$ variations in sedimentary archives can be misinterpreted as changes in hydrology. Our dataset shows large variability in ϵ_{app} values within and among individual plant groups (Fig. 3), which generates large variations in $\varepsilon_{C29/C23}$ values in sediments (s.d. = 24‰, Fig. 5). Therefore, $\varepsilon_{C29/C23}$ values in sedimentary records are expected to vary in time even during periods of stable vegetation sources, but even more so during shifts in vegetations sources (Fig. 3 and Fig. 5). Thus, a predominant aquatic input of n- C_{23} -alkane to sedimentary archives has to be well constrained before interpreting changes in $\varepsilon_{C29/C23}$ values as changes in evapotranspiration or in precipitation regimes.

4.3. Global relationship between mid- and long-chain n-alkanes to environmental waters

Previous studies show that n- C_{29} and MAP δ^2 H values correlate well at a global scale (Sachse et al., 2012; McFarlin et al., 2019; Ladd et al., 2021), and our results do not depart from this relationship (Fig. 6A). However, while our δ^2 H measurements improve the relationships between n- C_{23} and n- C_{29} to environmental waters (McFarlin et al., 2019), they indicate that n- C_{23} δ^2 H values are likely also linked to those of MAP rather than lake water δ^2 H signatures (Fig. 7). Several possible factors might influence these relationships.

First, higher terrestrial plant input to sedimentary archives at a global scale must generally dominate the n- C_{23} pool (Sachse et al., 2012; Nelson et al., 2018; Liu and Liu, 2019). Higher terrestrial plant leaf-wax δ^2 H values at our sites show similar $\varepsilon_{C23/MAP}$ distributions to those detected in sediments, which are more positive than those detected for aquatic sources (Fig. 3). Second, lake water δ^2 H values during the spring closely track those of MAP with an average $\varepsilon_{\text{Lake/MAP}}$ of 10% (s.d. = 16%). Likewise, the global $\varepsilon_{\text{Lake/MAP}}$ MAP distribution has a mean of 9% (s.d. = 25%) (Fig. 7B), which indicates that, at a global level, lake water δ^2 H values are controlled by MAP δ^2 H values. Consequently, the relationships between sedimentary $\delta^2 H$ values of individual *n*-alkanes and those of MAP or lake water are driven by ε_{app} (Fig. 3 and Fig. 6). Therefore, the updated global dataset confirms that: (1) both $n-C_{23}$ and n- C_{29} are likely derived from higher terrestrial plants (Fig. 7), and (2) the global relationships between *n*-alkanes δ^2 H values and environmental waters are determined by ε_{app} (Fig. 6 and Fig. 7). We speculate that the scatter in the relationship between observed versus predicted lake water δ^2 H values (Fig. 7A) is the result of a dominant higher terrestrial plant input to sedimentary archives, which generates a poor relationship between n-C₂₃ and lake water δ^2 H values at sites where MAP and lake water δ^2 H values are decoupled (Cluett and Thomas, 2020; Thomas et al., 2020).

In agreement with previous results from lakes across North America (Huang et al., 2002), modeled MAP and measured lake water δ^2H and $\delta^{18}O$ values are strongly correlated and plot near the GMWL (Fig. 2). While some of the lake water δ^2H values deviate from the GMWL (Fig. 2A), suggesting varying degrees of evaporative enrichment, the average $\epsilon_{\text{Lake/MAP}}$ value of 10% suggests that lake water δ^2H values during the spring are on average 10%

more positive than modeled MAP δ^2 H values. We further show that both measured lake water and modeled MAP δ^2 H values significantly correlate with modeled seasonal precipitation δ^2 H values (Table 3) but have the strongest relationships with modeled spring δ^2 H values (Pearson's r = 0.82 and 0.89, respectively). A strong correlation between measured lake water and modeled spring precipitation δ^2 H values is expected because lake water at our sites were sampled during the spring season. However, the strong correlation (Pearson's r = 0.89) between MAP and spring season precipitation δ^2 H values suggests that MAP δ^2 H values at our sites are mainly controlled by spring precipitation δ^2 H values. Therefore, because MAP δ^2 H values are strongest correlated to spring precipitation δ^2 H values and because lake water δ^2 H values show the strongest correlation to MAP δ^2 H values (Pearson's r = 0.89), both lake water and MAP δ^2 H values at our sites carry a spring precipitation signal. Since leaf wax *n*-alkanes have been shown to track the δ^2 H signatures of source moisture during leaf-formation (Tipple et al., 2013). which is spring season at our sites, leaf wax n-alkanes in plants and sediments should track modeled MAP δ^2 H composition.

At a global level, lakes also track MAP δ^2 H signatures, although some sites show a clear decoupling between lake water and MAP δ^2 H values (i.e., extremely low or high $\epsilon_{Lake/MAP}$ values (Fig. 7B). Furthermore, the global $\varepsilon_{C29/C23}$ distribution supports the hypothesis that on a global scale, the dominant source for n- C_{23} in sedimentary archives is of higher terrestrial plant origin (Fig. 7B). A dominant terrestrial source of mid- and long-chain n-alkanes to sedimentary archives is also supported by the strong correlations between n- C_{29} and other mid-and long-chain n-alkanes (Fig. 7C and D) where slope and intercept values are representative of the $\varepsilon_{\text{C29/MAP}}$ values in terrestrial plants at our sites (Fig. 3). The scatter in the relationship between n- C_{23} and n- C_{29} (Fig. 7E) could suggest a mix of n- C_{23} sources (e.g., aquatic vs terrestrial), but the intercept of the relationship suggests a dominant terrestrial source. If the *n*-C₂₃-alkane in the global dataset was predominatly derived from aquatic submergent plants (or aquatic plants in general), then the intercept value between n- C_{29} and n- C_{23} δ^2 H values would be negative as our data shows that $n\text{-}C_{29}$ δ^2H values in terrestrial plants are more positive than the $n-C_{23}$ values in aquatic plants (Fig. 3 and Fig. 5).

 $n\text{-}C_{25}$ and $n\text{-}C_{27}$ $\delta^2\text{H}$ values also correlate significantly with $n\text{-}C_{29}$ $\delta^2\text{H}$ values suggesting that both mid- and long-chain n-alkanes in sediments are likely derived from higher terrestrial plants (Fig. 7D-E). Furthermore, the intercepts of the global correlations (Fig. 7C-E) agree with the ϵ_{app} distributions found by comparing sediments and angiosperm trees (Fig. 3).

Given large uncertainties in $\epsilon_{alkane/water}$ values within and among individual plant groups (Fig. 3, Table 4; also see Sachse et al., 2012; Liu and Liu, 2016) and the strong correlation between MAP and lake water $\delta^2 H$ values at our sites (Fig. 2) and at a global scale (Fig. 7B), even if the dominant source for n- C_{23} to sedimentary archives would be of aquatic origin, absolute differences between MAP and lake water $\delta^2 H$ values would be difficult to constrain except for sites where lake water $\delta^2 H$ values are not controlled by MAP $\delta^2 H$ values. Therefore, constraining n- C_{23} and n- C_{29} sources and the dominant processes controlling lake water $\delta^2 H$ values is critical for interpreting sedimentary $\epsilon_{C29/C23}$ values in lake sediments.

5. Conclusions

Comparisons of n-alkanes $\delta^2 H$ values in plants and sediments from across mid-latitude North America demonstrate that both mid- and long-chain n-alkanes (i.e., n- C_{23} and n- C_{29}) in lake sediments commonly derive from higher terrestrial plants. Most likely,

the dominant terrestrial leaf wax input to sedimentary archives is driven by terrestrial vegetation because terrestrial plants cover larger source areas and have higher rates of leaf wax production compared to aquatic plants. We show that ε_{app} values vary as a function of n-alkane chain length and individual plant groups, and that at our sites, n- C_{23} and n- C_{29} ϵ_{app} values in surface sediments parallel those observed in higher terrestrial plants (i.e., angiosperm trees and gymnosperm trees) rather than those observed in grasses or in aquatic plants. While these findings pertain to our North American dataset, $n-C_{23}$ and $n-C_{29}$ -alkanes are likely derived from higher terrestrial plants in all lakes with landscapes covered in shrubs and trees. Therefore, n- C_{23} δ^2H values should not be universally used as a proxy for lake water isotopic composition. Future studies should first take into account vegetation sources using other independent proxies such as pollen or δ^{13} C analyses to correctly interpret n- C_{23} δ^2 H values.

Similarities between $\varepsilon_{\rm app}$ in sediments, angiosperm and gymnosperm trees at our sites indicate a dominant higher-terrestrial plant leaf wax input to sedimentary archives, but also show that vegetation shifts between angiosperm and gymnosperm trees would not impact $\varepsilon_{\rm app}$ values. Consequently, changes in leaf wax δ^2 H composition preserved in sedimentary archives can be interpreted as changes in the δ^2 H values of source water, especially during vegetation shifts between angiosperm and gymnosperms tree communities. Grasses produce a significant exception, however, because $n\text{-}C_{29}$ δ^2 H values in grasses are on average 32% lower than in angiosperms and 26% lower than in gymnosperms. Therefore, n-alkanes source in sedimentary archives needs to be constrained before interpreting $n\text{-}C_{29}$ δ^2 H values as changes in precipitation δ^2 H values.

Data availability

Data associated with this article is avaliable through the Mountain Scholar repository.

Declaration of Competing Interest

The authors declare that they have no known competing financial interests or personal relationships that could have appeared to influence the work reported in this paper.

Acknowledgments

We thank Dr. Nemiah Ladd and two other anonymous reviewers for providing helpful comments that greatly improved our manuscript. We thank James G. Sanford, David T. Liefert and Laurie Grigg for field work assistance. This work was supported by the Roy J. Shlemon Center for Quaternary Studies at the University of Wyoming, by the Department of Geology and Geophysics at the University of Wyoming, and by the Microbial Ecology Collaborative Project at the University of Wyoming through the National Science Foundation grant EPS-1655726.

Research Data

Data associated with this article can be accessed at https://doi.org/10.15786/20126483.v2.

Appendix A. Supplementary material

Supplementary material to this article can be found online at https://doi.org/10.1016/j.gca.2022.11.001.

References

- Aichner, B., Herzschuh, U., Wilkes, H., Vieth, A., Böhner, J., 2010a. δD values of *n*-alkanes in Tibetan lake sediments and aquatic macrophytes–A surface sediment study and application to a 16 ka record from Lake Koucha. Org. Geochem. 41 (8), 779–790.
- Aichner, B., Herzschuh, U., Wilkes, H., 2010b. Influence of aquatic macrophytes on the stable carbon isotopic signatures of sedimentary organic matter in lakes on the Tibetan Plateau. Org. Geochem. 41 (7), 706–718.
- Aichner, B., Hilt, S., Périllon, C., Gillefalk, M., Sachse, D., 2017. Biosynthetic hydrogen isotopic fractionation factors during lipid synthesis in submerged aquatic macrophytes: Effect of groundwater discharge and salinity. Org. Geochem. 113, 10–16.
- Balascio, N.L., D'Andrea, W.J., Bradley, R.S., Perren, B.B., 2013. Biogeochemical evidence for hydrologic changes during the Holocene in a lake sediment record from southeast Greenland. The Holocene 23 (10), 1428–1439.
- Bhattacharya, T., Tierney, J.E., Addison, J.A., Murray, J.W., 2018. Ice-sheet modulation of deglacial North American monsoon intensification. Nat. Geosci. 11 (11), 848–852.
- Bowen, G.J., 2020: Gridded maps of the isotopic composition of meteoric waters. http://www.waterisotopes.org.
- Bush, R.T., McInerney, F.A., 2013. Leaf wax n-alkane distributions in and across modern plants: implications for paleoecology and chemotaxonomy. Geochim. Cosmochim. Acta 117, 161–179.
- Chikaraishi, Y., Naraoka, H., 2003. Compound-specific δD - $\delta 13C$ analyses of n-alkanes extracted from terrestrial and aquatic plants. Phytochemistry 63 (3), 361–371.
- Cluett, A.A., Thomas, E.K., 2020. Resolving combined influences of inflow and evaporation on western Greenland lake water isotopes to inform paleoclimate inferences. J. Paleolimnol., 1–18
- Craig, H., 1961. Isotopic variations in meteoric waters. Science 133 (3465), 1702–1703.
- Curtin, L., D'Andrea, W.J., Balascio, N., Pugsley, G., de Wet, G., Bradley, R., 2019. Holocene and Last Interglacial climate of the Faroe Islands from sedimentary plant wax hydrogen and carbon isotopes. Quat. Sci. Rev. 223, 105930.
- Diefendorf, A.F., Freeman, K.H., Wing, S.L., Graham, H.V., 2011. Production of n-alkyl lipids in living plants and implications for the geologic past. Geochim. Cosmochim. Acta 75 (23), 7472–7485.
- Diefendorf, A.F., Freimuth, E.J., 2017. Extracting the most from terrestrial plantderived n-alkyl lipids and their carbon isotopes from the sedimentary record: A review. Org. Geochem. 103, 1–21.
- Diefendorf, A.F., Sberna, D.T., Taylor, D.W., 2015. Effect of thermal maturation on plant-derived terpenoids and leaf wax n-alkyl components. Org. Geochem. 89,
- Dion-Kirschner, H., McFarlin, J.M., Masterson, A.L., Axford, Y., Osburn, M.R., 2020. Modern constraints on the sources and climate signals recorded by sedimentary plant waxes in west Greenland. Geochim. Cosmochim. Acta 286, 336–354.
- Duan, Y., Wu, Y., Cao, X., Zhao, Y., Ma, L., 2014. Hydrogen isotope ratios of individual *n*-alkanes in plants from Gannan Gahai Lake (China) and surrounding area. Org. Geochem. 77, 96–105.
- Feakins, S.J., Peters, T., Wu, M.S., Shenkin, A., Salinas, N., Girardin, C.A., Bentley, L.P., Blonder, B., Enquist, B.J., Martin, R.E., Asner, G.P., 2016. Production of leaf wax *n*-alkanes across a tropical forest elevation transect. Org. Geochem. 100, 89–100.
- Feakins, S.J., Wu, M.S., Ponton, C., Galy, V., West, A.J., 2018. Dual isotope evidence for sedimentary integration of plant wax biomarkers across an Andes-Amazon elevation transect. Geochim. Cosmochim. Acta 242, 64–81.
- Ficken, K.J., Li, B., Swain, D.L., Eglinton, G., 2000. An n-alkane proxy for the sedimentary input of submerged/floating freshwater aquatic macrophytes. Org. Geochem. 31 (7–8), 745–749.
- Freimuth, E.J., Diefendorf, A.F., Lowell, T.V., Wiles, G.C., 2019. Sedimentary *n*-alkanes and n-alkanoic acids in a temperate bog are biased toward woody plants. Org. Geochem. 128. 94–107.
- Gao, L., Hou, J., Toney, J., MacDonald, D., Huang, Y., 2011. Mathematical modeling of the aquatic macrophyte inputs of mid-chain n-alkyl lipids to lake sediments: Implications for interpreting compound specific hydrogen isotopic records. Geochim. Cosmochim. Acta 75 (13), 3781–3791.
- Gao, L., Zheng, M., Fraser, M., Huang, Y., 2014. Comparable hydrogen isotopic fractionation of plant leaf wax n-alkanoic acids in arid and humid subtropical ecosystems. Geochem. Geophys. Geosyst. 15 (2), 361–373.
- He, D., Ladd, S.N., Saunders, C.J., Mead, R.N., Jaffé, R., 2020. Distribution of *n*-alkanes and their δ2H and δ13C values in typical plants along a terrestrial-coastal-oceanic gradient. Geochim. Cosmochim. Acta 281, 31–52.
- Hollister, K.V., Thomas, E.K., Raynolds, M.K., Bültmann, H., Raberg, J.H., Miller, G.H., Sepúlveda, J., 2022. Aquatic and terrestrial plant contributions to sedimentary plant waxes in a modern Arctic lake setting. J. Geophys. Res.: Biogeosci. 127 (8). e2022IG006903.
- Huang, Y., Shuman, B., Wang, Y., Webb III, T., 2002. Hydrogen isotope ratios of palmitic acid in lacustrine sediments record late Quaternary climate variations. Geology 30 (12), 1103–1106.
- Jetter, R., Kunst, L., Samuels, A.L., Riederer, M., Müller, C., 2006. Biology of the plant cuticle. Composit. Plant Cuticular Waxes, 145–181.
- Jiang, J., Meng, B., Liu, H., Wang, H., Kolpakova, M., Krivonogov, S., Song, M., Zhou, A., Liu, W., Liu, Z., 2021. Water depth control on n-alkane distribution and organic carbon isotope in mid-latitude Asian lakes. Chem. Geol. 565, 120070.

- Ladd, S.N., Maloney, A.E., Nelson, D.B., Prebble, M., Camperio, G., Sear, D.A., Hassall, J. D., Langdon, P.G., Sachs, J.P., Dubois, N., 2021. Leaf wax hydrogen isotopes as a hydroclimate proxy in the tropical Pacific. J. Geophys. Res.: Biogeosci. 126 (3). e2020[G005891.
- Liefert, D.T., Shuman, B.N., Parsekian, A.D., Mercer, J.J., 2018. Why are some rocky mountain lakes ephemeral? Water Resour. Res. 54 (8), 5245–5263.
- Liu, X., Feakins, S.J., Dong, X., Xue, Q., Marek, T., Leskovar, D.I., Neely, C.B., Ibrahim, A. M., 2017. Experimental study of leaf wax n-alkane response in winter wheat cultivars to drought conditions. Org. Geochem. 113, 210–223.
- Liu, H., Liu, W., 2016. n-Alkane distributions and concentrations in algae, submerged plants and terrestrial plants from the Qinghai-Tibetan Plateau. Org. Geochem. 99, 10–22.
- Liu, H., Liu, W., 2019. Hydrogen isotope fractionation variations of *n*-alkanes and fatty acids in algae and submerged plants from Tibetan Plateau lakes: Implications for palaeoclimatic reconstruction. Sci. Total Environ. 695, 133925.
- McFarlin, J.M., Axford, Y., Masterson, A.L., Osburn, M.R., 2019. Calibration of modern sedimentary $\delta 2H$ plant wax-water relationships in Greenland lakes. Quat. Sci. Rev. 225, 105978.
- Nelson, D.B., Ladd, S.N., Schubert, C.J., Kahmen, A., 2018. Rapid atmospheric transport and large-scale deposition of recently synthesized plant waxes. Geochim. Cosmochim. Acta 222, 599–617.
- Nichols, J.E., Booth, R.K., Jackson, S.T., Pendall, E.G., Huang, Y., 2006. Paleohydrologic reconstruction based on n-alkane distributions in ombrotrophic peat. Org. Geochem. 37 (11), 1505–1513.
- Nichols, J.E., Walcott, M., Bradley, R., Pilcher, J., Huang, Y., 2009. Quantitative assessment of precipitation seasonality and summer surface wetness using ombrotrophic sediments from an Arctic Norwegian peatland. Quat. Res. 72 (3), 443–451.
- Overpeck, J.T., Webb III, T., Prentice, I.C., 1985. Quantitative interpretation of fossil pollen spectra: dissimilarity coefficients and the method of modern analogs. Quat. Res. 23 (1), 87–108.
- Pagani, M., Pedentchouk, N., Huber, M., Sluijs, A., Schouten, S., Brinkhuis, H., Damsté, J.S.S., Dickens, G.R., 2006. Arctic hydrology during global warming at the Palaeocene/Eocene thermal maximum. Nature 442 (7103), 671–675.
- Peaple, M.D., Tierney, J.E., McGee, D., Lowenstein, T.K., Bhattacharya, T., Feakins, S.J., 2021. Identifying plant wax inputs in lake sediments using machine learning. Org. Geochem. 156, 104222.
- PRISM Climate Group, 2019. Oregon State University, http://prism.oregonstate.edu, created June 2019.
- Puleo, P.J., Axford, Y., McFarlin, J.M., Curry, B.B., Barklage, M., Osburn, M.R., 2020. Late glacial and Holocene paleoenvironments in the midcontinent United States, inferred from Geneva Lake leaf wax, ostracode valve, and bulk sediment chemistry. Quat. Sci. Rev. 241, 106384.
- R Core Team, 2018. R: A language and environment for statistical computing. R Foundation for Statistical Computing, Vienna, Austria. https://www.R-project.
- Rach, O., Brauer, A., Wilkes, H., Sachse, D., 2014. Delayed hydrological response to Greenland cooling at the onset of the Younger Dryas in western Europe. Nat. Geosci. 7 (2), 109–112.
- Rach, O., Kahmen, A., Brauer, A., Sachse, D., 2017. A dual-biomarker approach for quantification of changes in relative humidity from sedimentary lipid D/ H ratios. Clim. Past 13 (7), 741–757.
- Sachse, D., Radke, J., Gleixner, G., 2004. Hydrogen isotope ratios of recent lacustrine sedimentary *n*-alkanes record modern climate variability. Geochim. Cosmochim. Acta 68 (23), 4877–4889.
- Sachse, D., Radke, J., Gleixner, G., 2006. δD values of individual n-alkanes from terrestrial plants along a climatic gradient-Implications for the sedimentary biomarker record. Org. Geochem. 37 (4), 469–483.
- Sachse, D., Gleixner, G., Wilkes, H., Kahmen, A., 2010. Leaf wax n-alkane δD values of field-grown barley reflect leaf water δD values at the time of leaf formation. Geochim. Cosmochim. Acta 74 (23), 6741–6750.
- Sachse, D., Billault, I., Bowen, G.J., Chikaraishi, Y., Dawson, T.E., Feakins, S.J., Freeman, K.H., Magill, C.R., McInerney, F.A., Van Der Meer, M.T., Polissar, P., 2012. Molecular paleohydrology: interpreting the hydrogen-isotopic composition of lipid biomarkers from photosynthesizing organisms. Annu. Rev. Earth Planet. Sci. 40, 221–249.
- Schartman, A.K., Diefendorf, A.F., Lowell, T.V., Freimuth, E.J., Stewart, A.K., Landis, J. D., Bates, B.R., 2020. Stable source of Holocene spring precipitation recorded in leaf wax hydrogen-isotope ratios from two New York lakes. Quat. Sci. Rev. 240, 106357.
- Schefuß, E., Schouten, S., Schneider, R.R., 2005. Climatic controls on central African hydrology during the past 20,000 years. Nature 437 (7061), 1003–1006.
- Schimmelmann, A., Sessions, A.L., Mastalerz, M., 2006. Hydrogen isotopic (D/H) composition of organic matter during diagenesis and thermal maturation. Annu. Rev. Earth Planet. Sci. 34, 501–533.
- Seki, O., Meyers, P.A., Yamamoto, S., Kawamura, K., Nakatsuka, T., Zhou, W., Zheng, Y., 2011. Plant-wax hydrogen isotopic evidence for postglacial variations in delivery of precipitation in the monsoon domain of China. Geology 39 (9), 875–878
- Sessions, A.L., 2016. Factors controlling the deuterium contents of sedimentary hydrocarbons. Org. Geochem. 96, 43–64.
- Sessions, A.L., Sylva, S.P., Summons, R.E., Hayes, J.M., 2004. Isotopic exchange of carbon-bound hydrogen over geologic timescales. Geochim. Cosmochim. Acta 68 (7), 1545–1559.

- Thomas, E.K., Hollister, K.V., Cluett, A.A., Corcoran, M.C., 2020. Reconstructing Arctic precipitation seasonality using aquatic leaf wax $\delta^2 H$ in lakes with contrasting residence times. Paleoceanogr. Paleoclimatol. 35 (7). e2020PA003886.
- Tierney, J.E., Pausata, F.S., deMenocal, P.B., 2017. Rainfall regimes of the Green
- Sahara. Sci. Adv. 3 (1), e1601503. Tierney, J., Russell, J., Sinninghe Damsté, J., Huang, Y., Verschuren, D., 2011. Late Quaternary behavior of the East African monsoon and the importance of the Congo Air Boundary. Quat. Sci. Rev. 30 (7–8), 798–807.
- Tipple, B.J., Berke, M.A., Doman, C.E., Khachaturyan, S., Ehleringer, J.R., 2013. Leafwax n-alkanes record the plant-water environment at leaf flush. Proc. Natl. Acad. Sci. 110 (7), 2659-2664.
- Wang, Z., Liu, H., Cao, Y., 2018. Choosing a suitable ϵ w-p by distinguishing the dominant plant sources in sediment records using a new Pta index and estimating the paleo- δDp spatial distribution in China. Org. Geochem. 121, 161–168.
- Yang, H., Huang, Y., 2003. Preservation of lipid hydrogen isotope ratios in Miocene lacustrine sediments and plant fossils at Clarkia, northern Idaho, USA. Org. Geochem. 34 (3), 413-423.